HHS Public Access

Author manuscript

Lung Cancer. Author manuscript; available in PMC 2019 April 01.

Published in final edited form as:

Lung Cancer. 2018 April ; 118: 83–89. doi:10.1016/j.lungcan.2018.01.013.

What CT characteristics of lepidic predominant pattern lung adenocarcinomas correlate with invasiveness on pathology?

Emily A. Aherne[a], **Andrew J. Plodkowski**[a], **Joseph Montecalvo**[b], **Sumar Hayan**[a], **Junting Zheng**[c], **Marinela Capanu**[c], **Prasad S. Adusumilli**[d], **William D. Travis**[b], and **Michelle S. Ginsberg**[a]

[a]Department of Radiology, Memorial Sloan Kettering Cancer Center, 1275 York Ave, New York, NY 10065

[b]Department of Histopathology, Memorial Sloan Kettering Cancer Center, 1275 York Ave, New York, NY 10065

[c]Department of Epidemiology and Biostatistics, Memorial Sloan Kettering Cancer Center, 1275 York Ave, New York, NY 10065

[d]Department of Cardiothoracic Surgery, Memorial Sloan Kettering Cancer Center, 1275 York Ave, New York, NY 10065

Abstract

Objectives—The International Association for the Study of Lung Cancer, American Thoracic Society and European Respiratory Society lung adenocarcinoma classification in 2011 defined three lepidic predominant patterns including adenocarcinoma in situ, minimally invasive adenocarcinoma and lepidic predominant adenocarcinoma. We sought to correlate the radiology and pathology findings and identify any computed tomography (CT) features which can be associated with invasive growth.

Materials and Methods—An institutional review board approved, retrospective study was conducted evaluating 63 patients with resected, pathologically confirmed, adenocarcinomas with predominant lepidic patterns. Preoperative CT images of the nodules were assessed using quantitative and qualitative radiographic descriptors while blinded to pathologic sub-classification and size. Maximum diameter was measured after evaluation of the axial, sagittal and coronal planes. Radiologic – pathologic associations were examined using Fisher's exact test, the Kruskal-Wallis test and the Spearman correlation coefficient (ρ).

Results and Conclusion—Increasing maximum diameter of the whole lesion (ground glass and solid component) on CT was significantly associated with invasiveness (p=0.003), as was the maximum pathologic specimen diameter (p=0.008). Larger diameter of the solid component on CT was also found in lepidic predominant adenocarcinoma compared to minimally invasive

Corresponding author: Emily A. Aherne, 1275 York Ave, New York, NY 10065, emily.aherne@gmail.com.

adenocarcinoma (median 10.5 vs 2mm, p=0.005). More invasive tumors had higher visual estimated percentage solid component compared to whole lesion measurement on CT (p=0.014). CT and pathologic measurements were positively correlated, although only moderately (ρ =0.66) for the maximum whole lesion size and fair (ρ =0.49) for solid/invasive component maximum measurements. Larger whole lesion size and solid component size of lepidic predominant pattern adenocarcinomas are associated with lesion invasiveness, although radiologic and pathologic lesion measurements are only fair-moderately positively correlated.

Keywords

Lung adenocarcinoma; Lepidic predominant adenocarcinoma; Computed tomography; Radiology

1. Introduction

Lung cancer remains the second most commonly diagnosed major cancer for both men and women in the United States and the most common cause of cancer death for both sexes, accounting for 1 in 4 cancer deaths. The American Cancer Society estimates that in 2017, there will be 222,500 new cases of lung cancer and 155,870 deaths from lung cancer [1]. Of all histological subtypes of lung cancer, adenocarcinoma is the most common, occurring in approximately 40% of cases [2].

In 2011, the International Association for the Study of Lung Cancer, American Thoracic Society and European Respiratory Society defined three new sub-classifications of lepidic predominant pattern adenocarcinomas in order to integrate advances across multiple disciplines including not only pathology but medical oncology, molecular biology and radiology: adenocarcinoma in situ (AIS), minimally invasive adenocarcinoma (MIA) and non-mucinous lepidic predominant adenocarcinoma (LPA) [3]. In 2015, these sub-classifications were adopted by the World Health Organization [4]. Most recently, in 2017, the 8th edition lung cancer TNM classification incorporated the sub-classifications and made corresponding revisions to the T component of tumor, node, and metastasis (TNM) designation for lung cancer [5–7].

The change in pathologic classification requires an evaluation of the radiologic-pathologic correlation for optimal classification of these new lesions. As AIS and MIA categories were proposed based on evidence that patients would have a 100% or near-100% disease-free survival, respectively, if completely resected, it is vital that they can also be accurately identified and characterized on imaging. Data from our group suggest that even LPA have an excellent prognosis with 90% disease-free survival, and recurrence is associated with high risk features such as micropapillary component, visceral pleural or vascular invasion and close margins.[8] The purpose of this study was to determine the CT features of lepidic predominant tumors which correlate with histologic features of invasive growth.

2. Materials and Methods

2.1 Patient Population

This retrospective study was approved by the Institutional Review Board with a waiver of informed consent and was compliant with the Health Insurance Portability and Accountability Act. A review was performed to identify consecutive patients with resected, histopathologically confirmed lepidic predominant pattern tumors over a two year period from April 1, 2014, to March 23, 2016. We included all patients whose pre-operative CT imaging was performed up to a maximum of 2 months prior to surgery and which were available for evaluation in the picture archiving and communications system (GE Centricity, Chicago, IL). We excluded one patient in whom the lesion which was described on the pathology report but could not be definitely identified on CT.

2.2 CT Image Acquisition

We reviewed CT studies performed at our institution as well as those from outside institutions. We included studies performed with and without intravenous contrast. Imaging was performed with slice thickness ranging between 1.0 – 2.5 mm (axial plane), 2.0 - 3.0 mm (coronal plane) and 2.5 – 3.0 mm (sagittal plane) as we included outside studies.

CT studies performed at our institution included a single phase non-contrast or contrast-enhanced study with coverage from the base of the neck to include the adrenal glands inferiorly. It was performed with the patient in full inspiration on a multidetector CT (Discovery CT750HD, Lightspeed 16 and VCT, GE Healthcare, Chicago, IL). The following scan parameters were used: pitch/table speed = 0.984 to 1.375/27.50 to 39.37 mm; auto mA = 120 to 380; noise index = 12.5 to 16; rotation time = 0.5 s; injection to scan delay, if applicable = 40 s. Post-contrast arterial phase CT images were obtained following the administration of 80 mL iodinated contrast (Omnipaque 300, GE Healthcare, NJ) at 2.5 mL/sec. Axial slices were reconstructed at both 5.0 mm and 1.25 mm intervals using both soft tissue and lung algorithms. Multiplanar reconstructions were acquired in the coronal and sagittal planes with a 2.5 mm slice thickness on soft tissue windows. Post-processing was used to reconstruct these reconstructions using the lung algorithm with edge enhancement prior to analysis.

2.3 Image Analysis

Pre-operative CT images of the nodules were independently assessed using quantitative and qualitative radiographic descriptors by a radiology fellow (EA) blinded to pathologic sub-classification and size. All features were then reviewed in consensus reading with two attending thoracic radiologists (AP, MG) with 4 and 21 years radiology experience post–fellowship, respectively. All three readers reached a consensus on all lesions.

Lesions were evaluated for location including (a) anatomical lobar site and (b) central vs peripheral, where central was defined as any lesion contacting a central bronchus to the lobar level and peripheral was defined as any lesion beyond this level.

Lesions were also evaluated for size (in mm), measured on lung windows as the longest axis for length and then taking the longest perpendicular axis for width (Figure 1). The size in maximum perpendicular axis was measured on axial, coronal and sagittal reconstructed images. The presence or absence of a solid component was carefully evaluated taking care to exclude mass-like appearance of blood vessels or airways passing through the lesion. Unifocality and multifocality of the solid component was recorded and each solid component was again measured in perpendicular axes on each planar reconstruction (Figure 2). The single largest diameter of both the whole lesion and solid component and the plane of the reconstruction on which it was measured were also recorded.

The contour of the solid component was characterized as round/oval (sphere/ovoid with clearly defined smooth margins), lobulated (slightly irregular, rounded margins) or spiculated (solid lesion with linear extensions into the adjacent lung parenchyma). A visual estimate was made of the percentage volume of the solid component in relation to the volume of the whole lesion and categorized into 0% - no solid component, 1-25%, 26-50% and >50% (Figure 3).

2.4 Histopathological Analysis

Inclusion criteria for lesions examined this study were: 1) resection cases in which the entire tumor was examined (lobectomy, segmentectomy, and wedge resection), 2) a diagnosis of non-mucinous adenocarcinoma (AIS, MIA, or LPA), and 3) a predominantly lepidic pattern of growth (i.e. tumor cells growing along pre-existing alveolar walls making up the largest percentage of the tumor by microscopic measurement). Slides were re-reviewed in all cases by a histopathology fellow (JM) with supervision by a thoracic pathologist (WT). All patterns of adenocarcinoma (lepidic, solid, micropapillary, papillary, and acinar) were recorded in 5% increments. The total tumor sizes were measured microscopically or grossly according to previously described methods [7].

When the invasive focus could not be identified and measured in a single focus on one slide and measured with a ruler, the invasive size was estimated by multiplying the total percentage of the invasive components times the total size of the tumor. Other recorded features included the presence of fibroelastotic scars within the tumors (and the measurement of the scar), and the presence of multicentric invasion.

2.5 Statistical Analysis

Gender and radiographic features including maximum lesion size, maximum invasive component size, contour, percent of solid component on CT (0%, 1-25%, 26-50%, >50%), and presence of scar on pathologic specimen were associated with histology type (AIS, MIA, or LPA) using Fisher's exact test or the Kruskal-Wallis test. To evaluate correlation of whole lesion (WL) size and solid component (SOL-C) size on CT with pathologic whole lesion size and invasive component size on pathology, the Spearman correlation coefficient (ρ) was estimated considering the skewed distribution and the 95% confidence interval (CI) was calculated by using Fisher's z transformation. The receiver operation characteristic (ROC) analysis was performed to differentiate MIA and LPA using the SOL-C. A cutoff value of SOL-C size was selected based on the Youden index which maximizes the

combination of the sensitivity and the specificity. The empirical area under the curve (AUC), the sensitivity and the specificity at the cut off value were calculated.

3. Results

3.1 Patient demographics and CT parameters

Out of a total of 64 patients who met the inclusion criteria, 1 patient was excluded because the lesion could not be definitely identified on the CT. Thus, the total number of patients included in the final analysis was 63. They had a median age of 71 years (range, 40-86 years). 46 (73%) of the patients were female. 54 (85.7%) of the CT studies reviewed were performed at our institution with the remainder performed externally and uploaded to the PACS for review. 34 (54%) CT studies evaluated were performed without intravenous contrast. Axial slice thickness ranged from 1.0 – 3.0 mm, 58 studies (92.1%) included series with 1.25 mm slice thickness. Sagittal and coronal slice thickness ranged from 2.5 – 3.0 mm and 2.0 – 3.0 mm, respectively. Sagittal reconstructions were not available in 3 (4.8%) CT studies.

3.2 Pathologic Subtype and Location

Of the 63 lesions evaluated 4 (6.3%) were AIS, 27 (42.9%) were MIA and 32 (50.8%) were LPA (Figure 4). All lesions were peripherally located on CT. Anatomic lesion location was right upper lobe 22 (34.9%), left upper lobe including the lingula 17 (27%), left lower lobe 13 (20.6%), right lower lobe 8 (12.7%) and middle lobe 3 (4.8%). A scar was present in 10 (15.9%) lesions on histopathologic analysis.

3.3 Lesion Size and Morphology – Correlations between CT and Pathologic Findings

WL size was larger on CT than on pathology in 62/63 (98%) of lesions. SOL-C size on CT is larger than invasive component size on pathology in 34/63 (54%) of lesions, smaller in 23/63 (37%) of lesions and equal in 6/63 (10%) of lesions. Mean CT measurements of both WL size and SOL-C size were larger than mean pathologic measurements: WL mean was 27.6 mm (SD = 12.6) on CT vs.17 mm (SD = 8.9) on pathology; SOL-C mean was 7.4 mm (SD = 7.9) on CT vs. invasive component mean of 4.8 mm (SD = 3.3) on pathology. While there was a moderate positive correlation between the maximum diameter on CT and maximum diameter on pathology for WL ($\rho = 0.66$, 95%CI: 0.49, 0.78), SOL-C (CT)/ invasive (pathologic) components demonstrated fair positive correlation ($\rho = 0.49$, 95%CI: 0.27, 0.66).

We also demonstrated a significant association between WL size both radiologically and pathologically and lesion invasiveness. None of the AIS lesions had a solid component, although we have a small sample size. Larger tumors are more likely to show an invasive component. A significant association was also identified between the size of the SOL-C radiologically and lesion invasiveness identified by histology. When using SOL-C size to differentiate LPA and MIA the AUC was 0.708 (95%CI: 0.574-0.841). Based on Youden index, which maximized the combination of sensitivity and specificity, a cut-off value of 7.5 mm was found with a sensitivity of 0.719 (95%CI: 0.533-0.863,23/32) and a specificity of 0.704 (95%CI: 0.498-0.862, 19/27). The accuracies were moderate. (Table 1).

The maximum WL diameter measured on any plane, determined after measurement of the lesion on all three planes, was not always seen on the axial plane, as traditionally measured on CT but was seen on various planes dependent on the lesion morphology: axial 26 lesions (41.3%), sagittal 20 lesions (31.7%) and coronal 17 lesions (27%). Similarly the SOL-C maximum diameter was seen on various planes: axial 24 lesions (61.5%), sagittal 6 lesions (15.4 %) and coronal 9 lesions (23.1%).

The visually estimated percentage SOL-C on CT was significantly associated with lesion invasiveness, p = 0.014 (Table 2). The contour of the SOL-C, when present, was not significantly correlated with lesion invasiveness (Table 3).

A scar was present pathologically in 10/63 (16%) lesions. In 10 lesions with a scar, the median size difference between the SOL-C and the invasive component on pathology was 1.5 mm (IQR −1.75~4.28). In the 53 lesions without a scar, the median size difference was 1 mm (IQR −2~5). There was no statistical difference between the two groups (p=0.873). Thus in our study population, the presence of a scar was not significant cause of the size discrepancy between CT and pathology measurements.

4. Discussion

In our study, the size of the SOL-C as measured on CT correlated with the lesion invasiveness, as described by the most recent classification system described by the International Association for the Study of Lung Cancer, American Thoracic Society and European Respiratory Society in 2011 and adopted by the 2015 World Health Organization Classification and the 8th edition of the American Joint Committee on Cancer staging guidelines [3, 6, 9]. Tumor size is one of the strongest predictors of outcome in lung cancer [10, 11]. Furthermore, in lung adenocarcinoma, it has been demonstrated that the radiographic diameter of the SOL-C of a pulmonary small nodule on CT predicts overall survival better than WL diameter [12]. The Fleischner recommendations for management of sub-solid pulmonary nodules detected on CT are based on size [4]. Accurately measuring a lesion is vital in the staging of lung cancer patients to best select the appropriate management. Traditionally on CT the maximum dimension of the ground glass component is measured and, when present, the maximum dimension of the SOL-C is also measured. Tumor size for TNM staging should be made according to the single maximum diameter whether measured radiologically or pathologically [6, 7]. Our data show that the largest diameter of the lesion is not always measurable on the axial slice reconstructions; for example, we found the maximum SOL-C was best measured in other (coronal or sagittal) planes in 38.5% of cases.

An alternative, quantitative method of measuring sub-solid pulmonary nodules is volumetry [13–15]. To the best of our knowledge, it has not been proven superior to conventional measurements and is more labor intensive. However, we hypothesize that a visual estimation of percentage SOL-C of the WL could be a novel, time effective method of estimating the invasiveness of a lesion (Figure 3). Interestingly, the visual estimation we performed was associated with invasiveness of the lesion in this study population (p = 0.014). Further studies would need to be performed with a larger sample size, as well as evaluation with

intra- and inter-reader variability, to prove the efficacy of this method, which could potentially save valuable time during image analysis as it is quicker to perform than accurate multiplanar measurements.

Lesions with multifocal SOL-Cs are more challenging for the radiologist. There is no consensus as to the most accurate method of measurement. Several methods have been proposed for the measurement of these lesions including a technique proposed for microinvasive breast cancer which is to measure the largest solid focus and describe of the other foci in the report without measurement [4]. It is also possible to report each SOL-C individually or to sum the individual components together to provide an overall measurement. Kadota et al used this approach when determining the invasive component of part-solid adenocarcinomas on pathologic slides [8]. They measured all the invasive components and expressed their sum as a percentage of the overall tumor size. At present, the maximum diameter of the largest component is usually measured in line with most recent recommendations [7]. However, in our study, provisional results suggest that a subjective visual estimated percentage of the SOL-C as a percentage of the WL was correlated with lesion invasiveness. This would be particularly useful in these lesions with multifocal SOL-Cs.

It has been shown previously that there is a statistically significant difference between mean tumor diameter as measured by CT and on pathology gross specimen [16, 17]. This was again demonstrated in our study where the mean WL and SOL-C measurements were larger on CT than on pathologic examination (Figure 5). There was a positive correlation between the two (moderate and fair for WL and SOL-C, respectively). The reduced correlation in the SOL-C lesions may in part be explained by the overall smaller size of the lesions being measured compared to WL size. Possible reasons for the size discrepancy include the fact that pathologists have difficulty appreciating the lepidic component of lung adenocarcinomas on gross examination. In addition, the resected specimens are not aerated whereas patients are imaged by CT in full inspiration. Another factor is the fixation of specimens in formalin which can cause crenation [18, 19]. This lesion measurement discrepancy has implications for staging, particularly in patients being considered for more aggressive managements including resection. Inflation of specimens at the time of frozen section may improve correlation between pathologic radiologic size [20–22]. However, although this is performed on occasion, it is time consuming and thus not a routine procedure in clinical practice.

Many other studies have correlated CT findings of sub-solid pulmonary nodules with their pathologic findings [23–25]. The ground glass component of the lesion tends to correlate with the lepidic component on pathology [3]. It is also possible to have pure ground glass nodule with an invasive component pathologically [4]. In a study performed by Kim et al to identify factors that affected likelihood of tumor growth, the only predictor for the growth of ground glass nodules was the presence of a solid component [26]. We demonstrated a strong positive correlation between presence and size of the SOL-C and lesion invasiveness. Our ROC analysis suggested a cut-off of 7.5 mm to differentiate between MIA and LPA but this had just moderate accuracy. Further studies, with a larger study population would be required to validate this finding.

Although the solid component in a part-solid nodule seen by CT has a greater chance of having an invasive component on histologic examination, a benign scar or a fibrous scar harboring a stromal invasive component should also be considered [27]. Scar was present in 16% of lesions. In our study population, the presence of a scar was not a significant cause of the size discrepancy between CT and pathology measurements.

Beyond size measurements, other CT characteristics we reviewed included lesion location and morphology. All lesions evaluated in our study had a peripheral location, with an upper lobe predominance that is typical for adenocarcinomas. In the literature, round, smooth nodules are associated with benignity for primary lung malignancies but commonly seen in metastases. A lobulated contour implies some irregular growth and spiculated lesions are suspicious for malignancy.[28, 29] However, we did not identify a significant association between invasiveness and the contour of the solid component in this study, possibly related to sample size.

Our study has several limitations. It is a retrospective study with a relatively small sample size. Information regarding the specific surgical indication in each case was not available for review. Since these are recent cases, we did not have enough followup to perform survival analysis. Lesions were measured on CT in three reconstructed planes: axial, sagittal and coronal. The reconstructed slices in the sagittal and coronal planes were thicker than the axial plane both within our institution and on the outside studies. CT images are traditionally reconstructed in this manner to decrease the overall size of the imaging file for storage purposes. This can result in slightly less accurate measurements on the sagittal and coronal images compared to the axial images, however they are usually of diagnostic quality and warrant review when evaluating for the longest lesion diameter measurement [17]. Pathologists most commonly measure the lesion in the longest diameter and are less constrained by plane of view, although they are affected by the plane of the lesion transection. Our cases were evaluated in consensus by three radiologists which meant it was not possible to evaluate the inter-observer variability for the imaging appearances and measurements specific to these small lesions, although previously reported intra- and inter-observer variability in CT measurements in oncology specifically addressing lung nodules found that intra- and inter-observer variability rates are similar for lesions of assorted sizes and contour [30].

In conclusion, we demonstrated a positive correlation between presence and size of the SOL-C in lepidic predominant pattern lung adenocarcinomas as measured on CT and pathologic lesion invasiveness as described in the 8th edition of the AJCC staging manual. The contour of the solid component was not significantly associated with invasiveness but approached it.

Acknowledgments

This research was funded in part through the NIH/NCI Cancer Center Support Grant P30 CA008748. The funding source had no involvement in the study design; the collection, analysis and interpretation of data; in the writing of the report; or in the decision to submit the article for publication. We also wish to acknowledge Joanne Chin for her role in formatting the paper for publication.

Abbreviations

AIS	adenocarcinoma in situ
PathologyCI	confidence interval
CT	computed tomography
MIA	minimally invasive adenocarcinoma
LPA	lepidic predominant adenocarcinoma
WL	whole lesion
SOL-C	solid component
TNM	tumor, node, and metastasis

References

1. Siegel RL, Miller KD, Jemal A. Cancer Statistics, 2017. CA: a cancer journal for clinicians. 2017; 67(1):7–30. [PubMed: 28055103]
2. Meza R, Meernik C, Jeon J, Cote ML. Lung cancer incidence trends by gender, race and histology in the United States, 1973-2010. PloS one. 2015; 10(3):e0121323. [PubMed: 25822850]
3. Travis WD, Brambilla E, Noguchi M, Nicholson AG, Geisinger KR, Yatabe Y, Beer DG, Powell CA, Riely GJ, Van Schil PE, Garg K, Austin JH, Asamura H, Rusch VW, Hirsch FR, Scagliotti G, Mitsudomi T, Huber RM, Ishikawa Y, Jett J, Sanchez-Cespedes M, Sculier JP, Takahashi T, Tsuboi M, Vansteenkiste J, Wistuba I, Yang PC, Aberle D, Brambilla C, Flieder D, Franklin W, Gazdar A, Gould M, Hasleton P, Henderson D, Johnson B, Johnson D, Kerr K, Kuriyama K, Lee JS, Miller VA, Petersen I, Roggli V, Rosell R, Saijo N, Thunnissen E, Tsao M, Yankelewitz D. International association for the study of lung cancer/american thoracic society/european respiratory society international multidisciplinary classification of lung adenocarcinoma. Journal of thoracic oncology: official publication of the International Association for the Study of Lung Cancer. 2011; 6(2):244–85.
4. (!!! INVALID CITATION !!!).
5. Amin, MB.Edge, SB.Greene, FL., et al., editors. Cancer Staging Manual. 8. Springer International Publishing; New York:
6. Brierley, JD.Gospodarowicz, MK., Wittekind, C., editors. TNM Classification of Malignant Tumours. 8. Wiley-Blackwell; Oxford, UK; Hoboken, NJ: 2017.
7. Travis WD, Asamura H, Bankier AA, Beasley MB, Detterbeck F, Flieder DB, Goo JM, MacMahon H, Naidich D, Nicholson AG, Powell CA, Prokop M, Rami-Porta R, Rusch V, van Schil P, Yatabe Y. The IASLC Lung Cancer Staging Project: Proposals for Coding T Categories for Subsolid Nodules and Assessment of Tumor Size in Part-Solid Tumors in the Forthcoming Eighth Edition of the TNM Classification of Lung Cancer. Journal of thoracic oncology: official publication of the International Association for the Study of Lung Cancer. 2016; 11(8):1204–23.
8. Kadota K, Villena-Vargas J, Yoshizawa A, Motoi N, Sima CS, Riely GJ, Rusch VW, Adusumilli PS, Travis WD. Prognostic significance of adenocarcinoma in situ, minimally invasive adenocarcinoma, and nonmucinous lepidic predominant invasive adenocarcinoma of the lung in patients with stage I disease. The American journal of surgical pathology. 2014; 38(4):448–60. [PubMed: 24472852]
9. Travis, WD.Brambilla, E.Burke, AP., et al., editors. WHO Classification of Tumours of the Lung, Pleura, Thymus and Heart. 4. IARC Press; Lyon, France: 2015.
10. Rami-Porta R, Bolejack V, Crowley J, Ball D, Kim J, Lyons G, Rice T, Suzuki K, Thomas CF Jr, Travis WD, Wu YL. The IASLC Lung Cancer Staging Project: Proposals for the Revisions of the T Descriptors in the Forthcoming Eighth Edition of the TNM Classification for Lung Cancer.

Journal of thoracic oncology: official publication of the International Association for the Study of Lung Cancer. 2015; 10(7):990–1003.

11. de Groot PM, Carter BW, Cuellar SLBetancourt, Erasmus JJ. Staging of lung cancer. Clinics in chest medicine. 2015; 36(2):179–96. vii–viii. [PubMed: 26024599]
12. Burt BM, Leung AN, Yanagawa M, Chen W, Groth SS, Hoang CD, Nair VS, Shrager JB. Diameter of Solid Tumor Component Alone Should be Used to Establish T Stage in Lung Adenocarcinoma. Annals of surgical oncology. 2015; 22(Suppl 3):S1318–23. [PubMed: 26228108]
13. Oda S, Awai K, Murao K, Ozawa A, Yanaga Y, Kawanaka K, Yamashita Y. Computer-aided volumetry of pulmonary nodules exhibiting ground-glass opacity at MDCT. AJR American journal of roentgenology. 2010; 194(2):398–406. [PubMed: 20093602]
14. Oda S, Awai K, Murao K, Ozawa A, Utsunomiya D, Yanaga Y, Kawanaka K, Yamashita Y. Volume-doubling time of pulmonary nodules with ground glass opacity at multidetector CT: Assessment with computer-aided three-dimensional volumetry. Academic radiology. 2011; 18(1): 63–9. [PubMed: 21145028]
15. de Hoop B, Gietema H, van de Vorst S, Murphy K, van Klaveren RJ, Prokop M. Pulmonary ground-glass nodules: increase in mass as an early indicator of growth. Radiology. 2010; 255(1): 199–206. [PubMed: 20123896]
16. Lampen-Sachar K, Zhao B, Zheng J, Moskowitz CS, Schwartz LH, Zakowski MF, Rizvi NA, Kris MG, Ginsberg MS. Correlation between tumor measurement on Computed Tomography and resected specimen size in lung adenocarcinomas. Lung cancer (Amsterdam, Netherlands). 2012; 75(3):332–5.
17. Ridge CA, Huang J, Cardoza S, Zabor EC, Moskowitz CS, Zakowski MF, Ginsberg MS. Comparison of multiplanar reformatted CT lung tumor measurements to axial tumor measurement alone: impact on maximal tumor dimension and T stage, AJR. American journal of roentgenology. 2013; 201(5):959–63. [PubMed: 24147464]
18. Tran T, Sundaram CP, Bahler CD, Eble JN, Grignon DJ, Monn MF, Simper NB, Cheng L. Correcting the Shrinkage Effects of Formalin Fixation and Tissue Processing for Renal Tumors: toward Standardization of Pathological Reporting of Tumor Size. Journal of Cancer. 2015; 6(8): 759–66. [PubMed: 26185538]
19. Hsu PK, Huang HC, Hsieh CC, Hsu HS, Wu YC, Huang MH, Hsu WH. Effect of formalin fixation on tumor size determination in stage I non-small cell lung cancer. The Annals of thoracic surgery. 2007; 84(6):1825–9. [PubMed: 18036892]
20. Isaka T, Yokose T, Ito H, Imamura N, Watanabe M, Imai K, Nishii T, Woo T, Yamada K, Nakayama H, Masuda M. Comparison between CT tumor size and pathological tumor size in frozen section examinations of lung adenocarcinoma. Lung cancer (Amsterdam, Netherlands). 2014; 85(1):40–6.
21. Xu X, Chung JH, Jheon S, Sung SW, Lee CT, Lee JH, Choe G. The accuracy of frozen section diagnosis of pulmonary nodules: evaluation of inflation method during intraoperative pathology consultation with cryosection. Journal of thoracic oncology: official publication of the International Association for the Study of Lung Cancer. 2010; 5(1):39–44.
22. Myung JK, Choe G, Chung DH, Seo JW, Jheon S, Lee CT, Chung JH. A simple inflation method for frozen section diagnosis of minute precancerous lesions of the lung. Lung cancer (Amsterdam, Netherlands). 2008; 59(2):198–202.
23. Kim HY, Shim YM, Lee KS, Han J, Yi CA, Kim YK. Persistent pulmonary nodular ground-glass opacity at thin-section CT: histopathologic comparisons. Radiology. 2007; 245(1):267–75. [PubMed: 17885195]
24. Aoki T, Nakata H, Watanabe H, Nakamura K, Kasai T, Hashimoto H, Yasumoto K, Kido M. Evolution of peripheral lung adenocarcinomas: CT findings correlated with histology and tumor doubling time, AJR. American journal of roentgenology. 2000; 174(3):763–8. [PubMed: 10701622]
25. Lee KH, Goo JM, Park SJ, Wi JY, Chung DH, Go H, Park HS, Park CM, Lee SM. Correlation between the size of the solid component on thin-section CT and the invasive component on pathology in small lung adenocarcinomas manifesting as ground-glass nodules. Journal of thoracic oncology: official publication of the International Association for the Study of Lung Cancer. 2014; 9(1):74–82.

26. Kim HS, Lee HJ, Jeon JH, Seong YW, Park IK, Kang CH, Kim KB, Goo JM, Kim YT. Natural history of ground-glass nodules detected on the chest computed tomography scan after major lung resection. The Annals of thoracic surgery. 2013; 96(6):1952–7. [PubMed: 24083798]

27. Yamada N, Kusumoto M, Maeshima A, Suzuki K, Matsuno Y. Correlation of the solid part on high-resolution computed tomography with pathological scar in small lung adenocarcinomas. Japanese journal of clinical oncology. 2007; 37(12):913–7. [PubMed: 18211981]

28. Furuya K, Murayama S, Soeda H, Murakami J, Ichinose Y, Yabuuchi H, Katsuda Y, Koga M, Masuda K. New classification of small pulmonary nodules by margin characteristics on high-resolution CT. Acta radiologica (Stockholm, Sweden: 1987). 1999; 40(5):496–504.

29. Seemann MD, Seemann O, Luboldt W, Bonel H, Sittek H, Dienemann H, Staebler A. Differentiation of malignant from benign solitary pulmonary lesions using chest radiography, spiral CT and HRCT. Lung cancer (Amsterdam, Netherlands). 2000; 29(2):105–24.

30. McErlean A, Panicek DM, Zabor EC, Moskowitz CS, Bitar R, Motzer RJ, Hricak H, Ginsberg MS. Intra- and interobserver variability in CT measurements in oncology. Radiology. 2013; 269(2): 451–9. [PubMed: 23824993]

Highlights

- Increasing maximum diameter on CT was significantly associated with invasiveness.
- More invasive tumors had a higher visually estimated percentage solid component.
- Radiologic and pathologic measurements are fair-moderately positively correlated.

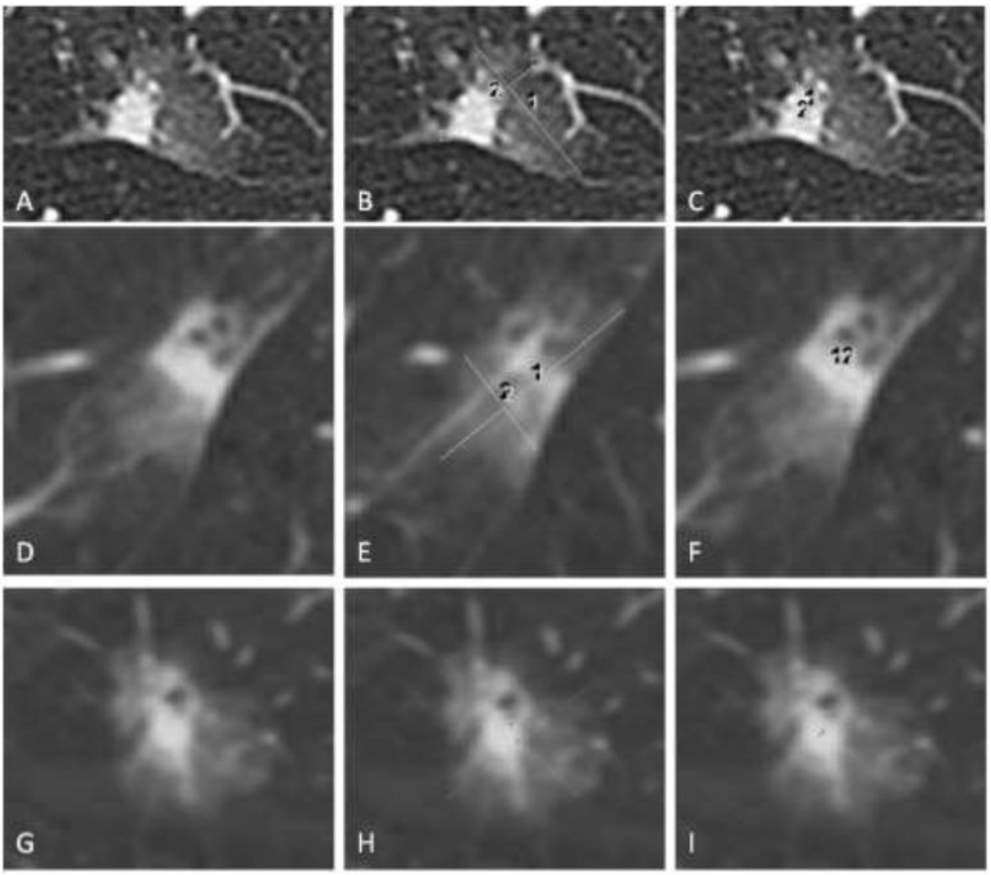

Figure 1.

Measuring lesions on CT. (A-C) Axial CT images of a subsolid lesion with (B) measurement of the whole lesion in maximum long axis and a perpendicular measurement and (C) measurement of the solid component in maximum long axis and a perpendicular measurement. (D-F) The lesion and measurements taken in the sagittal plane. (G-I) The lesion and measurements taken in the coronal plane.

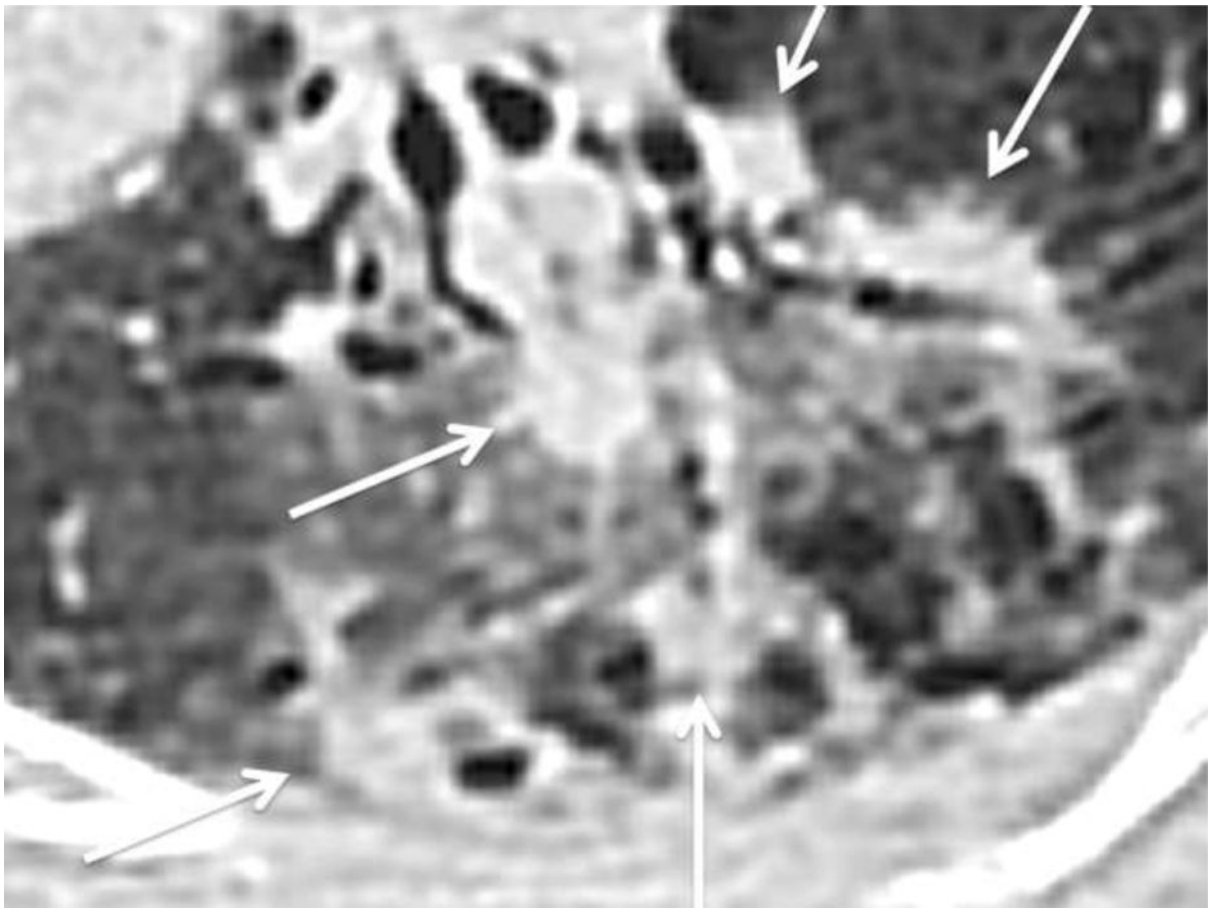

Figure 2.
Subsolid nodule with multifocal solid components. Axial CT image on lung windows demonstrating a subsolid lesion with multifocal solid components (arrows).

Figure 3.
Visual Percentage estimation. Example axial CT image on lung windows of a multifocal lesion with estimated 25-50% solid component.

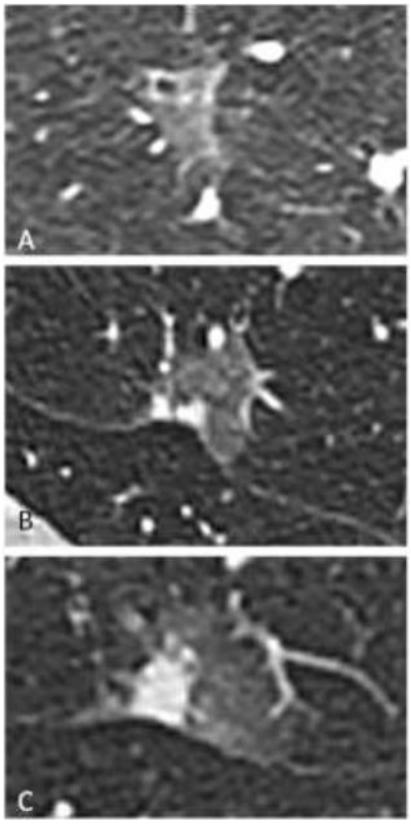

Figure 4.

Lesion subtype example images. Axial CT images on lung windows of (A) adenocarcinoma in situ, (B) minimally invasive adenocarcinoma and (C) lepidic predominant adenocarcinoma.

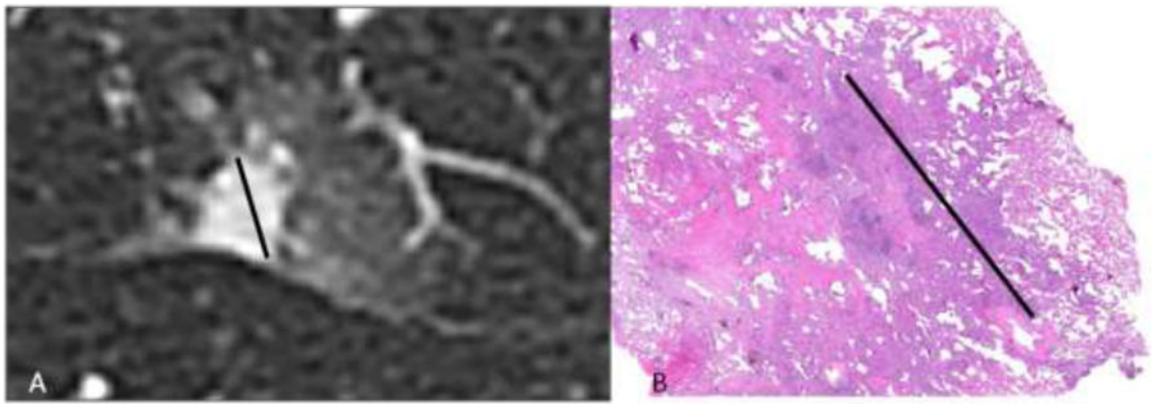

Figure 5.

Radiologic-pathologic size measurement discrepancy. (A) Axial CT image of a subsolid nodule where the solid component measures 1.1 cm. (B) Histopathologic slide of the same lesion stained with haemotoxylin and eosin on low power with the invasive component measured at 0.8 cm.

Table 1

Both the radiologic and pathologic WL and SOL-C/invasive component size increased with lesion invasiveness. None of the AIS lesions had a solid component, although we have a small sample size.

	Histopathologic Sub-type			p Value
	AIS (n=4)	MIA (n=27)	LPA (n=32)	
Rad max WL size (mm)	15.5 (10, 25)	23 (14, 56)	28.5 (10, 75)	0.003 *
Path WL size (mm)	9.5 (8, 18)	13 (7, 52)	17.5 (4, 46)	0.008 *
Rad max SOL-C size (mm)	0 (0, 0)	2 (0, 22)	10.5 (0, 32)	0.005 *Ɨ
Path invasive component size, (mm)	0 (0, 0)	3 (0.3, 10)	7 (1, 13)	<.001 *Ɨ

Note: AIS = Adenocarcinoma in situ, MIA = Minimally invasive adenocarcinoma, LPA = Lepidic predominant adenocarcinoma;

* significant at P<0.05;

Ɨ Comparison was done between MIA and LPA.

Table 2

Radiologic percentage visual estimation of the solid component in relation to the whole lesion was significantly associated with pathologic subtype.

% of invasive component on CT	Histopathologic Sub-type			
	AIS (n=4)	MIA (n=27)	LPA (n=32)	p Value
				0.014
0%	4 (100%)	13 (48.1%)	7 (21.9%)	
1-25%	0 (0%)	8 (29.6%)	6 (18.8%)	
26-50%	0 (0%)	1 (3.7%)	8 (25%)	
>50%	0 (0%)	5 (18.5%)	11 (34.4%)	

Author Manuscript

Author Manuscript

Author Manuscript

Table 3

Contour of the solid component was not significantly associated with histopathologic subtype.

	Histopathologic Sub-type			
	AIS (n=4)	**MIA (n=27)**	**LPA (n=32)**	**p Value**
Contour				
				0.199
Round/Oval	0 (0%)	7 (50%)	6 (24%)	
Lobulated	0 (0%)	3 (2.4%)	5 (20%)	
Spiculated	0 (0%)	4 (28.6%)	14 (56%)	